3858–3865 *Nucleic Acids Research, 1996, Vol. 24, No. 19*

A new approach to overcome potassium-mediated inhibition of triplex formation

Fedor Svinarchuk[1,3,*], Dmitry Cherny[2,4], Arnaud Debin[1], Etienne Delain[2] and Claude Malvy[1]

[1]Laboratoire de Biochimie–Enzymologie and [2]Laboratoire Microscopie Cellulaire et Moleculaire, CNRS URA 147, Institute Gustave Roussy, rue Camille Desmoulins, 94805 Villejuif Cedex, France, [3]Department of Biochemistry, Novosibirsk Institute of Bioorganic Chemistry, 8 Prospect Lavrenteva, Novosibirsk 630090, Russia and [4]Institute of Molecular Genetics, RAS, Kurchatov's sq., Moscow 123182, Russia

Received April 16, 1996; Revised and Accepted August 9, 1996

ABSTRACT

G,A-containing purine oligonucleotides of various lengths form extremely stable and specific triplexes with the purine–pyrimidine stretch of the *vpx* gene [Svinarchuk,F., Monnot,M., Merle,A., Malvy,C. and Fermandjian,S. (1995) *Nucleic Acids Res.*, 22, 3742–3747]. The potential application of triple-helix-forming oligonucleotides (TFO) in gene-targeted therapy has prompted us to study triplex formation mimicking potassium concentrations and temperatures in cells. Triplex formation was tested by dimethyl sulphate (DMS) footprinting, gel-retardation, UV melting studies and electron microscopy. In the presence of 10 mM $MgCl_2$, KCl concentrations up to 150 mM significantly lowered both efficiency (triplex : initial duplex) and rate constants of triplex formation. The KCl effect was more pronounced for 11mer and 20mer TFOs than for 14mer TFO. Since the dissociation half-life for the 11mer TFO decreases from 420 min in the absence of monovalent cations to 40 min in the presence of 150 mM KCl, we suggest that the negative effect could be explained by a decrease in triplex stability. In contrast, for the 20mer TFO no dissociation of the triplex was observed during 24 h of incubation either in the absence of monovalent cations or in the presence of 150 mM KCl. We suppose that in the case of the 20mer TFO the negative effect of KCl on triplex formation is probably due to the self-association of the oligonucleotide in competitive structures such as parallel duplexes and/or tetraplexes. This negative effect may be overcome by the prior formation of a short duplex either on the 3′- or 5′-end of the 20mer TFO. We refer to these partial duplexes as 'zipper' TFOs. It was demonstrated that a 'zipper' TFO can form a triplex over the full length of the target, thus unzipping the short complementary strand. The minimal single-stranded part of the 'zipper' oligonucleotide which is sufficient to initiate triplex formation can be as short as three nucleotides at the 3′-end and six nucleotides at the 5′-end. We suggest that this type of structure may prove useful for *in vivo* applications.

INTRODUCTION

Short homopurine–homopyrimidine regions in DNA have attracted a great deal of attention in connection with their possible role in gene regulation in eukaryotes (1,2). These regions raise the possibility of manipulating gene expression, gene-targeted mutagenesis and inhibition of virus propagation through artificial triple helix formation (3–5). Recognition of DNA by triplex forming oligonucleotides (TFO) occurs by hydrogen bonding between oligonucleotide bases and purine bases in the major groove of duplex DNA. The triple helix formation arises in either of two patterns, termed the pyrimidine motif and the purine motif (6,7). To promote triplex formation with cytosine-containing oligonucleotides a slightly acidic environment is required. In contrast, the purine motif is pH-independent, so has been used far more often for successful *in vivo* inhibition of transcription. However, a growing number of publications report that triplexes involving guanine-rich oligonucleotides are inhibited by physiological ionic conditions, particularly by the presence of K^+ cations (8–10). It can be assumed that this effect is caused by the formation of the competitive structures, such as guanine quartets and parallel-stranded homoduplexes (8–10).

We have previously investigated the triplex formation by G,A-containing oligonucleotides of various lengths (from 11mer to 20mer) with a sequence of the c-*pim* promoter region and a highly conserved 20 bp-long purine–pyrimidine tract of the *vpx* gene of SIV and HIV-2 at 50 mM Na^+ concentration (11,12). Despite the high efficiency of triplex formation *in vitro*, we were unable to detect triplex formation inside the cell (13). Taking this into account, in the present work, *in vitro* studies have been extended to include physiological K^+ concentrations. It was found that an increase in Na^+ or K^+ concentration leads to a decrease in the rate of triplex formation and the level of guanine protection judged by DMS footprint experiments. This effect is more pronounced in the case of K^+. Based on the stability

*To whom correspondence should be addressed at: Laboratoire de Biochimie–Enzymologie, CNRS URA 147, Institut Gustave Roussy, rue Camille Desmoulins, 94805 Villejuif Cedex, France

measurements of the corresponding triplexes we suggest that the reasons for the decrease in guanine protection are different for the 11mer versus the longer oligonucleotides (14-, 17- and 20mer). For the 11mer TFO, the triplex is significantly destabilised by the increase of K^+ concentration, leading to less protection of guanines. For longer oligonucleotides, the data indicate that the increase of potassium concentration favours the formation of inter- and/or intramolecular structures which are stable at physiological temperature thus decreasing the effective concentration of TFOs. This consequently results in a lower efficiency of triplex formation. To avoid these self-association of the oligonucleotides the 20mer TFO was annealed with complementary oligonucleotides (from 10- to 17mers) matching either the 5′- or the 3′- end of the TFO. Thus preformed duplexes, named 'zipper' TFOs were able to form triplexes with the target sequence under our experimental conditions. The rate of triplex formation with 'zipper' oligonucleotides is practically independent of the K^+ or Na^+ concentration over a range of 0 to 150 mM. The 'zipper' TFOs containing 8 or 10 residues in a single-stranded form at the 3′-end have displayed the maximum efficiency and rate of triplex formation. Moreover these oligonucleotides form practically 'perfect' triplexes with the target sequence as evaluated by DMS footprinting. We suggest that 'zipper' TFOs may prove useful in gene targeted therapy based on triple helix formation.

MATERIALS AND METHODS

Oligonucleotide preparation

Oligonucleotides were synthesised on an Applied Biosystems 391A DNA synthesiser using the solid phase phosphoramidite procedure. They were precipitated with 10 vol of 3% solution of $LiClO_4$ in acetone and the pellets were washed with acetone, dried and dissolved in water. Concentrations were determined spectrophotometrically. Extinction coefficients were calculated by the extinction coefficients for the nucleotides and dinucleotide phosphates according to the equation given in Puglisi *et al.* (14). For gel-retardation assays oligonucleotides were purified by electrophoresis in a 20% denaturing polyacrylamide gel. After electrophoresis the oligonucleotides were eluted from the gel in 1 ml 0.2 M $LiClO_4$ solution during 12 h at 37 °C followed by a precipitation with 10 vol acetone. The 5′-end of the pyrimidine strand of the duplex was radiolabelled with [γ-^{32}P]ATP (Amersham) by T4 polynucleotide kinase (New England Biolabs) as per manufacturer's instructions. The oligonucleotide was labelled at a specific activity of 20 Ci/mmol. 'Zipper' oligonucleotides were prepared by heating of a 20mer TFO with an excess of the corresponding complementary oligonucleotide (molar ratio 1/1.2) at 95°C for 15 min and then the mixture was allowed to cool slowly down to room temperature.

Plasmid construction

The plasmid pVpx1 containing the polypurine stretch of the SIV *vpx* gene was made by inserting the oligonucleotides 5′-CTAGAC-CTGGAGGGGGAGGAGGAGGAGGTCCG-3′/5′-GATCCGG-ACCTCCTCCTCCTCCCCCTCCAGGT-3′ into the *Xba*I–*Bam*HI sites of the vector pBluescript II (Stratagene). All plasmids were grown in the XL1 Blue bacterial strain (Stratagene) and purified by CsCl gradient centrifugation (15).

DMS footprinting

To prepare a DNA fragment for modification by DMS the pVpx1 plasmid was cut with the *Cla*I restriction enzyme, 3′ labelled with the Klenow fragment of DNA polymerase I, and digested with the *Xho*I restriction enzyme. A larger labelled fragment (1.0 pmol) was dissolved in a 20 µl volume containing 50 mM MOPS, pH 7.2, 10 mM $MgAc_2$ and monovalent cations at the concentrations indicated in the legends of Figures 2 and 7. After addition of the TFO, the mixture was brought to 37°C for the time specified in the figure legends. Then 2 µl 5% DMS was added and the reaction was performed for 2 min at 25°C. The reaction was stopped by the addition of a 5 µl solution containing 10% mercaptoethanol, 1 mM EDTA and 0.1 M NaAc. After two precipitations in ethanol the samples were treated with 50 µl 10% piperidine at 95°C for 20 min, and the cleavage products were separated on a 6% denaturing polyacrylamide gel.

The level of guanine protection in DMS footprinting experiments for VPX20 and Zip2 TFO was measured by using a FUJIX BAS 1000 phosphoimager. Two regions of the targeted sequence, i.e. GGGGG and GGAGG, marked I_T and I_t on Figure 5A, respectively, were chosen for this purpose. A sequence close to the target sequence, marked I_c on Figure 5A, was chosen as a control. For each sequence the total intensities of five bands were measured in two runs of experiment: in the presence of TFO (A_T, A_t and A_c, respectively) and in its absence (C_T, C_t and C_c, respectively). These were further used for the calculation of guanine protection, X_T and X_t, respectively, according to the formula (given for I_T region):

$$X_T = 1 - (A_T/A_c)/(C_T/C_c)$$

where the term C_T/C_c represents the normalisation factor used to take into account possible variation in the quantity of the radioactivity, loaded on the gel. X_T and X_t were determined for various times for VPX20 and Zip2 TFOs (lanes 1–6 and 8–13 in Fig. 5, respectively). The same equation was used to determine the level of guanine protection in the sequence GGAGG.

UV spectroscopic temperature dependent melting studies

Absorbance of the oligonucleotide mixtures was measured at 258 nm as a function of temperature with an Uvicon 941 spectrophotometer equipped with a Bioblock Ministat cryothermostat and a Huber PD415 temperature programmer through software developed for T_m recording. The rate of temperature increase was 0.5°C/min. The buffer composition and oligonucleotide concentration are specified in the text. Before performing melting studies, all the samples were heated at 95°C for 15 min and then allowed to return slowly to room temperature.

Co-migration assay

After triplex formation a 50% glycerol solution was added to bring the solution to a 5% final concentration in glycerol, and the samples were loaded on a 1% agarose gel. Electrophoresis was performed at 3.5 V/cm at room temperature for 4 h in the presence of 20 mM Tris-acetate, 50 mM NaAc, 10 mM $MgAc_2$ and 1 µg/ml ethidium bromide. The quantity of the radioactivity bound to the targeted DNA was determined using a FUJIX BAS 1000 phosphoimager with flow-dried gel.

Rate of triplex formation as determined by a co-migration assay

To determine the rate of triplex formation, 2 µg plasmid pVpx1 (1 pmol) was incubated for various times with 10 pmol γ-^{32}P-labelled TFO (specific activity 20 Ci/mmol). The reaction was carried out in a 15 µl solution containing 10 mM $MgAc_2$, 20 mM Tris-acetate, pH 7.5, and 200 pmol of the unrelated oligonucleotide 5′-GAGGCGGCAGGGCGAGAGGC-3′ in order to avoid non-specific adsorption of the TFO to the tube walls. The concentration of K^+ is specified in the text. After co-migration, the amount of radioactively labelled oligonucleotide bound to the plasmid was determined using a FUJIX BAS 1000 phosphoimager.

Determination of the dissociation rate of the triplexes

Triplexes were preformed by overnight incubation at 37°C of 10 pmol pVpx1 plasmid DNA, linearised with *Cla*I, with 2 pmol of the TFO (specific activity 1000 Ci/mmol) in the presence of 10 mM $MgAc_2$, and 20 mM Tris-acetate, pH 7.5. The preformed triplex (1 pmol of the plasmid) was further incubated for different lengths of time with an excess (500 pmol) of the same non-labelled oligonucleotide in a 15 µl solution containing the same buffer and Na^+ or K^+ at the concentrations specified in the text. After performing a co-migration assay, the amount of radioactive labelled oligonucleotide bound to the plasmid was determined using a FUJIX BAS 1000 phosphoimager.

Electron microscopy (EM)

The oligonucleotide 5′-GGAGGAGGAGGAGGGGGAGG-3′-biotin (bio-VPX20) was purchased from GenSet (France). pVpx1 plasmid DNA was linearized with the *Kpn*I. For EM a procedure similar to that described by Cherny and co-workers (16,17) was used: 0.1 µg pVpx1/*Kpn*I plasmid DNA was incubated at 37°C for the desired time with bio-VPX-20 in a 10 µl volume, either in 10 mM Tris–HCl, pH 7.5, 50 mM NaCl, 10 mM $MgAc_2$ (buffer A) or in 20 mM Tris–HCl, pH 7.5, 10 mM NaCl, 150 mM KCl and 10 mM $MgAc_2$ (buffer B). Then the mixture was passed through a Superose 6 column equilibrated with buffer A, and streptavidin (Sigma) was added to DNA-containing fractions to a final concentration of 5–20 µg/ml (80–300 nM); after 10 min incubation at room temperature the gel filtration step was repeated. For the kinetic experiments aliquots were taken from the mixture and diluted 10-fold in buffer A; then streptavidin was immediately added at a 10-fold molar excess in comparison with the concentration of oligonucleotide. After 10 min incubation at room temperature the mixture was subjected to gel-filtration as above. A 5 µl aliquot was then applied to a carbon film glow-discharged in the presence of pentylamine vapours as described by Dubochet *et al.* (18), stained with an 0.5–1% aqueous solution of uranyl acetate and rotary shadowed with Tantalum/Tungsten with the electron gun of a Balzers MED 010 apparatus. The samples were observed with a Zeiss/LEO CEM-902 electron microscope in the annular dark-field mode using the technique described by Delain *et al.* (19, 20). Image recording and length measurements of DNA molecules were performed with the built-in Kontron image analyzer system and software. The efficiency of triplex formation was measured as a ratio of the number of DNA molecules with bound streptavidin in the right position to the total number of scored DNA molecules. Usually, 500–700 DNA molecules were scored for each experiment.

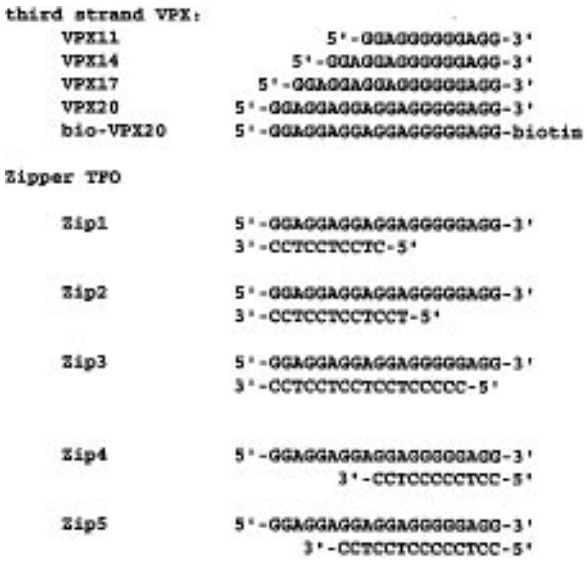

Figure 1. Sequences of the triplex-forming oligonucleotides targeted to a 20 bp polypurine/polypyrimidine region of the SIV and HIV-2 *vpx* gene. The third strand oligonucleotides were designed to bind in an antiparallel orientation when compared to the purine strand of the duplexes.

RESULTS

Purine–purine–pyrimidine triplex formation is affected by temperature and monovalent cations

DMS footprinting. The oligonucleotides used for the targeting of the *vpx* gene in the present experiments are listed in Figure 1. Triplex formation with the pVpx1 plasmid DNA in the buffer containing 50 mM Na^+ was monitored by a DMS footprinting assay (Fig. 2). DMS modifies the N7 position of guanines leading to phosphate backbone chain cleavage after treatment with piperidine. This reaction does not occur with the purines of the double-stranded DNA within a purine–purine–pyrimidine triplex due to formation of Hoogsteen base pairing (21). Figure 2 shows that the guanines located within the target sequences of all oligonucleotides tested (VPX11, VPX14, VPX17 and VPX20) are less affected by DMS treatment in comparison to those external to the corresponding targets suggesting that triplex is formed with each of the oligonucleotides under the experimental conditions used. In accordance with our previously published results (12), guanines within triplexes formed at 37°C were less protected over the full length of the TFO by longer oligonucleotides, especially at the 3′-end of the targeted sequence (Fig. 2, lanes 3–5). The pattern of protection changed when triplexes preformed at 37°C in the buffer containing 50 mM Na^+ were heated to 70°C for 3 min followed by DMS treatment at room temperature. In this case the observed protection corresponded well to the length of TFOs (Fig. 2, lanes 6–9).

The level of guanine protection was inversely dependent on K^+ or Na^+ concentration up to 150 mM. This effect is most pronounced for the 11-, 17- and 20mer oligonucleotides (data not shown).

Electron microscopy. In parallel, electron microscopy was used to detect the triplex formation by using a 3′-end biotinylated derivative of VPX20. The electron micrograph is presented in Figure 3A together with the corresponding histogram of location

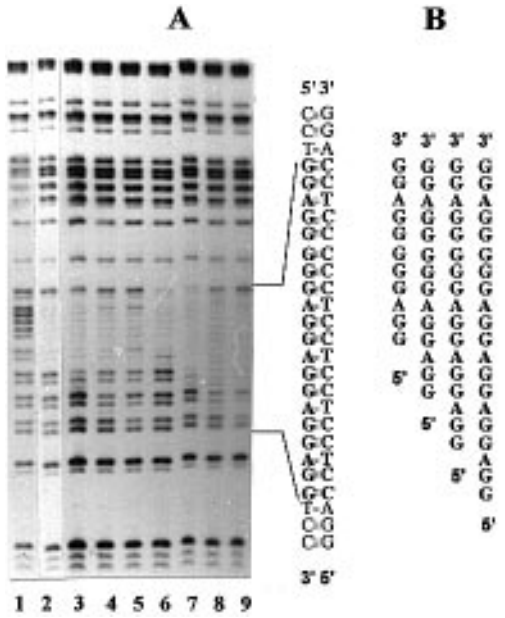

Figure 2. DMS footprinting experiments carried out with TFOs of different length. (**A**) Autoradiogram of a 6% polyacrylamide sequencing gel showing the results of DMS footprinting experiments carried out with TFOs (5 μM concentration) of increasing length after triplex formation at 37°C in the buffer containing 50 mM NaAc: lane 1, control oligonucleotide 5′-GAGGCGG-CAGGGCGAGAGGC-3′; lane 2, VPX11; lane 3, VPX14, lane 4, VPX17, lane 5, VPX20; lanes 6–9 correspond to the samples in the lanes 2–5 but after 3 min heating at 70°C. (**B**) Sequences of the TFOs used in lane 2–9.

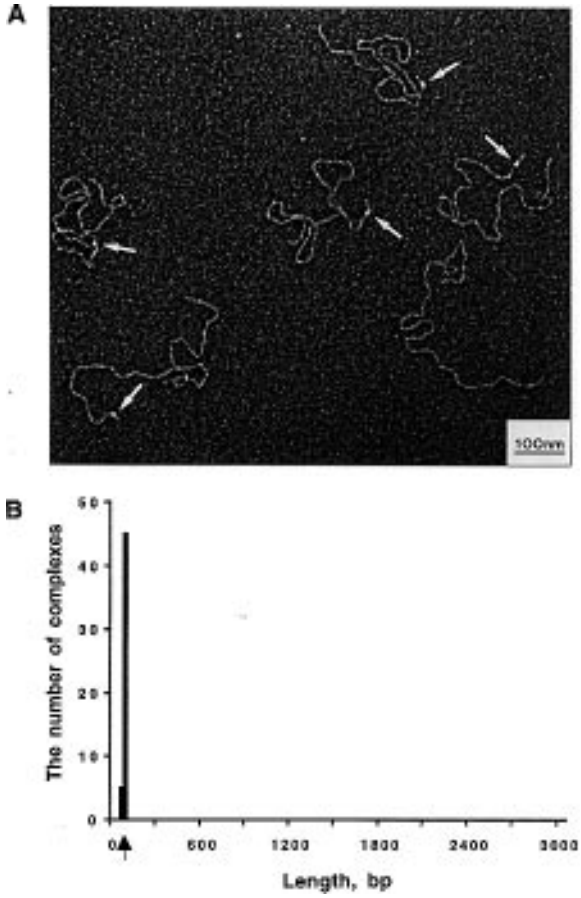

Figure 3. Electron microscopy visualisation of the triplex. The sites of triplex formation are seen as streptavidin molecules. (**A**) Micrograph of the complex bio-VPX20/pVpx-*Kpn*I/streptavidin. The arrows indicate streptavidin molecules. The triplex was obtained by the 'zipper' bio-VPX20. Micrograph was taken with the annular dark-field mode on rotary shadowed molecules. (**B**) Histogram of the distribution of bound strepavidin molecules over 50 DNA molecules. The position of the peak centre is 82 bp from the nearest end. The arrow indicates the position of the target (64–84 bp).

of bound streptavidin molecules along the length of the pVpx1/*Kpn*I plasmid DNA (Fig. 3B). The position of the peak on the histogram (83 bp from the nearest end) coincides with the position of the target sequence (64–84 bp from the same end) with an error ±15 bp. When the experiments were performed in the presence of 50 mM NaCl, the efficiency of triplex formation as measured by occupation of the target with streptavidin did not exceed 70%. Moreover, this value slightly decreased upon increasing the concentration of bio-VPX20 from 1 to 10 μM. Substitution of 50 mM NaCl by 150 mM KCl lowered the yield of the EM detectable triplexes to 15–20%. In agreement with DMS footprinting data, a short heating of the incubation mixture to 70°C for 3–5 min increased the yield of triplexes up to 55%. The high selectivity of this particular bio-TFO is indicated by the fact that for all levels of target sequence occupation studied (up to 80%), no non-specific interaction over the whole plasmid sequence was observed.

Half-life of triplex dissociation. The half-lives of the triplexes at 37°C in the absence of monovalent cations were 420 min for the 11mer oligonucleotide (VPX11) and more than 100 h for the others (VPX14, VPX17 and VPX20 respectively). At a 150 mM K^+ concentration, the corresponding values were respectively: 40 min for 11mer (VPX11), about 100 h for 14mer (VPX14) and more than 100 h for 17- and 20mer (VPX17 and VPX20). Electron microscopic examination of the complexes after passing through a gel-filtration column also confirmed that there was practically no decay of the triplexes with bio-VPX20 after 24 h of incubation at room temperature (data not shown).

These data suggest that the main reason for decrease in the protection of guanines by VPX11 upon increasing salt concentration is the lowering of the triplex stability. In contrast, the stability of the longer TFOs are virtually independent of salt concentration and protection pattern may be explained in another way. One possible explanation is that VPX14, VPX17 and VPX20 can form oligonucleotide species that are refractory to triplex formation. To examine this hypothesis we analysed by various methods the behaviour of VPX20 TFO for which the dependency of triplex formation from salt concentration was more pronounced than for other TFOs.

VPX20 structure: UV melting studies

To study possible inter-and/or intramolecular interactions, we performed melting studies of VPX20 TFO under conditions of different ionic strengths. In the presence of 10 mM $MgAc_2$ and 20 mM Tris-acetate, pH 7.5, the T_m was concentration-dependent, ranging from 36.0°C at 0.5 μM of oligonucleotide concentration to 42.5°C at 8 μM (Fig. 4). The addition of 50 mM KCl in the buffer produces melting profiles without pronounced transition.

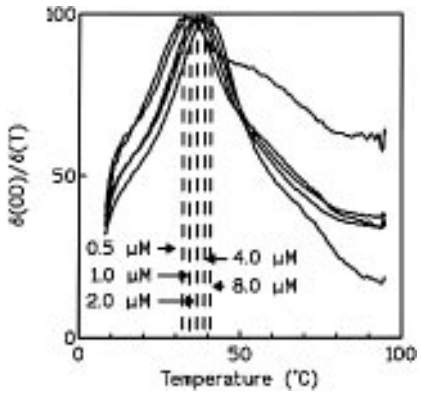

Figure 4. Derivatives of the melting temperature curves of the TFO VPX20. The buffer contained 10 mM $MgAc_2$, and 20 mM Tris-acetate, pH 7.5. Melting temperatures, which are determined as a maximum of each curve are indicated by the dotted lines and corresponding concentrations of the oligonucleotide are indicated by arrows.

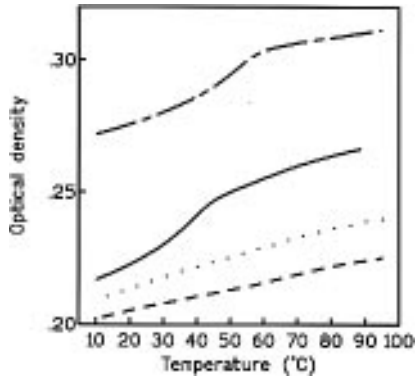

Figure 5. Melting temperature curves of the oligonucleotide VPX20 at 1 μM concentration. Solid line, run in the buffer containing 10 mM $MgAc_2$, 20 mM Tris-acetate, pH 7.5; dotted and dashed lines, the same buffer plus 50 or 150 mM KCl correspondingly; long-dash line, oligonucleotide VPX20 plus complementary 12mer oligonucleotide 5′-TCCTCCTCCTCC-3′ in the buffer containing 10 mM $MgAc_2$, 150 mM KCl and 20 mM Tris-acetate, pH 7.5.

The shape of the curves are independent of the KCl concentration from 50 to 150 mM KCl (Fig. 5).

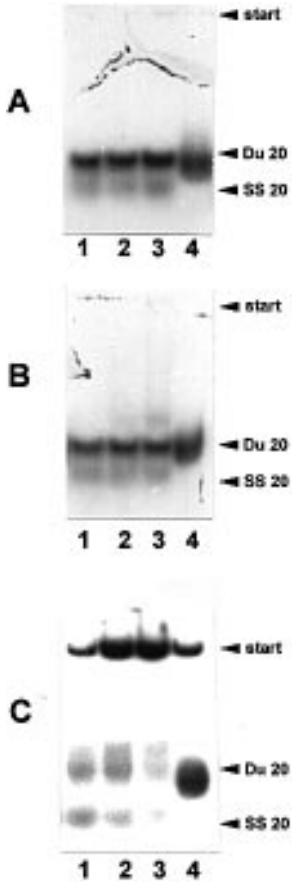

Figure 6. Autoradiogram of a 10% polyacrylamide non-denaturing gel showing the results of VPX20 self association after heating up to 90°C and slowly cooling in buffers of different composition. (**A**) 10 mM $MgAc_2$, 20 mM Tris-acetate, pH 7.5. (**B**) 10 mM $MgAc_2$, 50 mM NaAc, 20 mM Tris-acetate, pH 7.5. (**C**) 10 mM $MgAc_2$, 50 mM KAc, 20 mM Tris-acetate, pH 7.5. Lanes 1, 2 and 3 correspond to 0.5, 2 and 8 μM concentrations of the TFO respectively. Lane 4 corresponds to the TFO Zip2 (Fig. 1). For (A) and (B) electrophoresis was run in the buffer containing 10 mM $MgAc_2$, 50 mM NaAc, 20 mM Tris-acetate pH 7.5, and for (C) in the buffer containing 10 mM $MgAc_2$, 50 mM KAc, 20 mM Tris-acetate pH 7.5. SS20 indicates the position of the 5′-CCTCCTCCTCCTCCCCCTCC-3′ oligonucleotide. DU20 indicates the position of the 5′-CCTCCTCCTCCTCCCCCT-CC-3′/5′-GAGGCGGCAGGGCGAGAGGC-3′ duplex.

VPX20 structure: a non-denaturing gel assay

In order to determine whether self-association of VPX20 is responsible for the inhibition of triplex formation by monovalent cations we investigated the state of the oligonucleotide under triplex forming conditions by an electrophoretic mobility shift assay. Figure 6 shows that heating of the oligonucleotide solution with 10 mM $MgAc_2$ and 20 mM Tris-acetate, pH 7.5 at 95°C for 15 min followed by slow cooling to room temperature leads to the appearance of two bands upon non-denaturing gel electrophoresis (Fig. 6A, lanes 1–3). The mobility of the faster band coincides with the control pyrimidine-rich oligonucleotide 5′-CCTCCTC-CTCCTCCCCCTCC-3′ position which is indicated by an arrow SS 20 in Figure 6A. The second, slower band, migrates with the mobility corresponding to the duplex of VPX20 with its complementary strand (marked Du 20 in the Figure 6). The pattern remains the same when the concentration of the TFO increased from 0.5 to 8 μM (Fig. 6A, lanes 1–3). The appearance of the slowly migrating band can be attributed to the formation of the parallel purine/purine duplex previously described for GGA-containing oligonucleotides (10).

Addition of 50 mM NaAc to the incubation mixture leads to the formation of additional complexes which migrate more slowly than the duplex DU 20 (Fig. 6B, lanes 2 and 3). Addition of 50 mM KAc to the incubation mixture leads to more pronounced structural changes of the oligonucleotide (Fig. 6C), which are dependent on the TFO concentration. At a 0.5 μM oligonucleotide concentration the major part of the oligonucleotide is presented by two bands migrating as the single strand and the duplex oligonucleotides, but at 2 μM and 8 μM concentrations the major part of the oligonucleotide does not enter into the gel and is seen as a thick band in the well. The structure of this complex is unknown, but analysis using EM does not reveal the presence of high molecular weight complexes.

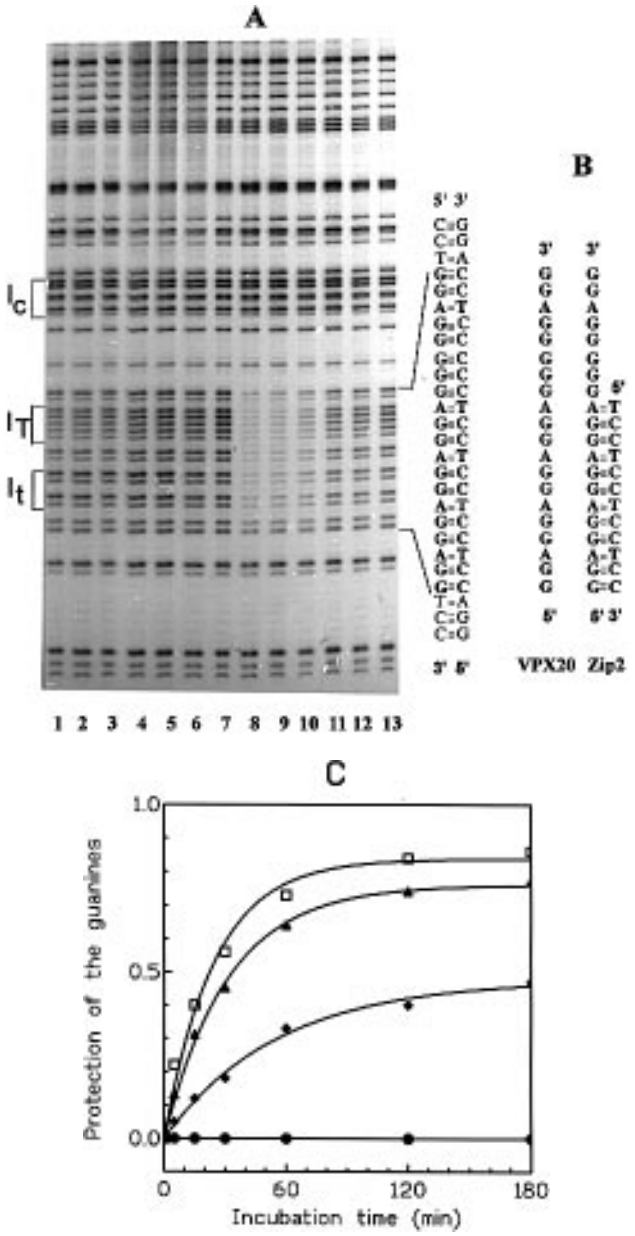

Figure 7. DMS footprinting experiments on the kinetic of triplex formation in the presence of 150 mM KCl for VPX20 (lanes 1–6) and Zip2 (lanes 8–13) TFOs. (**A**) Autoradiogram of a 6% polyacrylamide sequencing gel showing the results of DMS footprinting experiments carried out for different incubation time of the targeted DNA at 37°C with VPX20 (lanes from 1 to 6 correspond to 180, 120, 60, 30, 15 and 5 min of incubations); and with Zip2 (lanes from 8 to 13 correspond to 180, 120, 60, 30, 15 and 5 min of incubations). Lane 7, control oligonucleotide 5′-GAGGCGGCAGGGCGAGAGGC-3′. The TFOs concentration is 0.7 µM. (**B**) Sequences of the TFO used in the experiment. (**C**) Quantitative estimation of the relative protection of the guanines (see Materials and Methods for the details). Protection of the guanines in the sequence GGGGG: □ (Zip2) and ◆ (VPX20); protection of the guanines in the sequence GGAGG ▲ (Zip2) and ● (VPX20).

VPX20 structure: a 12mer complementary oligonucleotide decrease self-association in the VPX20 TFO

In order to avoid possible inter- and/or intramolecular interactions, VPX20 was annealed to a 12mer oligonucleotide, 5′-TCCTCCTC-CTCC-3′, which is complementary to the 5′-end of the TFO. Heating at 95°C for 15 min followed by slow cooling to room temperature of the purine TFO with a complementary strand, either in buffer without monovalent cations or in the presence of 50 mM NaAc, results in the formation of one major band most probably corresponding to the duplex formed between VPX20 and the 12mer (Fig. 6A and B, lane 4). Moreover, the addition of the 12mer to the VPX20 in buffer containing 50 mM NaAc eliminated the bands migrating more slowly than the duplex (Fig. 6B, lane 4). In the presence of 50 mM KAc and the highest concentration of the TFO tested (8 µM) the 12mer oligonucleotide substantially decreases the self-association of the oligonucleotide. This is shown by the decreased intensity of the band located in the well and the appearance of the major band with the mobility close to that of the marker duplex (Fig. 6C, lane 4).

Melting temperature studies showed that the addition of this 12mer oligonucleotide to VPX20 to the buffer containing 10 mM $MgAc_2$, 150 mM KAc and 20 mM Tris-acetate, pH 7.5 triggers a transition in the melting curves with T_m varying from 47.5 to 55.0°C for concentrations of oligonucleotides ranging from 0.5 to 8.0 µM (Fig. 5). Because these melting temperatures coincide with the melting temperatures of the duplex 5′-GGAGGAGGA-GGA-3′/5′-TTCTTCTTCTTC-3′ (data not shown), we suggest that addition of the 12mer to VPX20 leads to the Watson–Crick base pairing between these two oligonucleotides and thus prevents VPX20 self-association.

These results demonstrate that duplex formed between the 5′-end of VPX20 TFO significantly eliminate the self-association of VPX20 TFO. We named this partial duplex a ‘zipper’ TFO.

Kinetic analysis of triplex formation by VPX20 and its ‘zipper’ forms

As noted above the dissociation of the triplex formed by VPX20 is very slow ($t_{1/2}$ >100 h). This allowed us to use as a first approximation the following equation of triplex formation:

$$d[Tr]/dt = -d[D]/dt = k_{in}[D][O], \quad \mathbf{1}$$

where [Tr], [D] and [O] are the triplex, duplex and TFO concentrations, respectively. Since the oligonucleotide concentration in our experiments is 10 times the concentration of the target sequence, this second order reaction can be solved as a pseudo first order one:

$$[Tr]/[D^\circ] = Tr_\infty\{1 - \exp(-k_{in}[O]t)\}, \quad \mathbf{2}$$

where [D°] is the initial concentration of the target site, Tr_∞ is the fraction of the targeted sites occupied by the TFO when the reaction reaches the plateau. Estimates for k_{in} and for Tr_∞ were obtained by least squares fitting of kinetic data to the equation **2**. The kinetic data for VPX20 and ‘zipper’ oligonucleotide Zip2 were obtained by three methods.

(i) Footprinting experiments (Fig. 7). We estimated the rate of triplex formation for different parts of the target sequence: for the first stretch of five Gs and for the following sequence GGAGG. In Figure 7C one can see that equation **2** describes the process of triplex formation by ‘zipper’ TFO both for the stretch of five Gs and for the sequence GGAGG. The corresponding values for k_{in} and Tr_∞ are given in Table 1A. These values are lower for the GGAGG sequence in comparison to those for the GGGGG sequence. The k_{in} and Tr_∞ values for VPX20 determined by the footprint method for the five Gs sequence were two times lower than the corresponding values for Zip2 TFO (Table 1A). However

we did not see any footprint for the sequence GGAGG in the case of the VPX20 oligonucleotide (Fig. 7A and C).

(ii) Co-migration assay (Table 1B). The value of k_{in} determined on the basis of the co-migration assay indicates the total amount of oligonucleotide bound to the targeted plasmid but does not permit the observation of non-perfect triplexes. Nevertheless the footprinting and co-migration methods yield similar values for k_{in}.

(iii) Electron microscopy experiments. k_{in} estimated in the experiments with bio-VPX20 at 2 μM TFO concentration was found to be about $0.3 \pm 0.05 \times 10^3$ $M^{-1}s^{-1}$. Comparison of the Tr_∞ values for bio-VPX20, either pure ($Tr_\infty = 0.15$) or after duplex formation with the complementary 12mer oligonucleotide ($Tr_\infty = 0.80$), also confirmed the difference in triplex formation efficiency.

K_{in} and Tr_∞ for different types of 'zipper' oligonucleotides, estimated by the co-migration assay are given in Table 1B. Two generalizations can be made from these data. First, some of the 'zipper' oligonucleotides (numbers 1, 2 and 4) possess higher efficiency of triplex formation in comparison to VPX20. Second, 'zipper' oligonucleotides with complementary strand matching the 5′-end of TFO are faster in triplex formation when compared to those with the complementary strand matching the 3′-end. However there is no direct correlation between the rate of triplex formation k_{in} and its efficiency Tr_∞. For example, the value of Tr_∞ for Zip4 is very close to the unit but the rate is seven times less than for VPX20.

Zip3 and Zip5 TFOs give the lowest values as for k_{in} as well for Tr_∞. Nevertheless, the three nucleotides in a single-stranded form at the 3′-end (Zip3) or six nucleotides at the 5′-end (Zip5) promote triplex formation detectable by the co-migration assay.

DISCUSSION

Previously we found that the G,A-containing oligonucleotides targeted to the c-*pim* promoter region and to the *vpx* gene of SIV and HIV2 viruses form very stable triplexes at 50 mM Na^+ concentration. Melting temperatures of these triplexes were found to be higher than the corresponding values for double-stranded target sequences. Despite the high efficiency of triplex formation *in vitro*, we were unable to detect triplex formation inside the cell (13). Recent investigations have indicated that K^+ promotes the formation of oligonucleotide species refractory to triplex formation (8,10). Taking this into account, in the present work, *in vitro* studies have been extended to include physiological K^+ concentrations. An increase in Na^+ or K^+ concentration decreases the rate of triplex formation and the level of guanine protection as judged by DMS footprint experiments. These phenomena are more pronounced for K^+. We suggest that at least three processes might be responsible for these phenomena.

First, elevated concentration of the monovalent cations may change the parameters of interaction between the target sequence and TFOs at the triplet level. Because the stability of the triplex can be considered as a function of the stability of each triplet in the triplex, these parameters determine the minimum length of the stable triplex. In our case only the stability of the 11mer TFO was substantially decreased by the addition of K^+ up to 150 mM thus leading to less guanine protection. For the longer TFO, however, we did not see any substantial decrease in the stability of the triplexes at increased monovalent cation concentrations.

Second, DMS footprinting indicates that TFOs of a length of 14mer or more can simultaneously form a triplex with the targeted sequence and participate in additional intra- and/or intermolecular interactions. This in turn results in the appearance of non-perfect or 'degenerate' triplexes, in which only a part of the TFO interacts with the target sequence. These non-perfect triplexes are probably less stable than the correctly formed ones, but they could prevent 'perfect' triplex formation by other TFOs over the full target length. Ten times excess of initial TFO concentration in our experiments may result in full occupancy of the target site by the complexes of various stability while only a part of them yield the triplexes registered by any methods. This effect could explain the low value of Tr_∞ for VPX20 TFO in our kinetic measurements. The coexistence of perfect together with non-perfect triplexes has been already described for PNA oligomers (22).

Third, for longer oligonucleotides, the data indicate that the increase of potassium concentration favours the formation of inter- and/or intramolecular structures which are stable at physiological temperature. This, in their turn, can change the parameters of interaction between TFOs and their targets lowering the efficiency of triplex formation.

The negative effect of K^+ on triplex formation by guanosine-rich oligonucleotides has been described (8,10,23). Various explanations have been suggested to explain this phenomenon including formation of some oligonucleotide structures which are refractory to triplex formation (8,10) or which do not involve the self-association of TFO (23). In the latter case the authors tested self-association of the TFO by a co-migration assay in the presence of EDTA in the gel, when the triplex formation took place in the presence of 10 mM Mg^{2+}. From our experience, and others (10) the presence of Mg^{2+} may be crucial for the stability of the self-associated TFO structures. This may explain why the authors did not see oligonucleotide aggregates by their method. Also the difference in the TFO behaviour might be attributed to differences in oligonucleotide sequences.

Table 1. Parameters of the kinetic of triplex formation for various TFOs

			VPX20	zip1	zip2	zip3	zip4	zip5
A	GGGGG	K_{in}	0.43 ± 0.05		1.01 ± 0.10			
		Tr_∞	0.48 ± 0.02		0.84 ± 0.03			
	GGAGG	K_{in}	0.00		0.81 ± 0.05			
		Tr_∞			0.76 ± 0.01			
B		K_{in}	0.72 ± 0.18	0.58 ± 0.05	0.96 ± 0.05	>0.002	0.10 ± 0.02	0.002 ± 0.0005
		Tr_∞	0.53 ± 0.05	0.90 ± 0.03	0.86 ± 0.02	–	0.94 ± 0.05	

K_{in} is expressed in 10^3 $M^{-1}s^{-1}$. Tr_∞ is expressed as a ratio of triplex concentration after 3 h of incubation to the initial concentration of the target. (A) Data were obtained from footprinting experiments for two regions of the target GGGGG and GGAGG (see also Fig. 7). (B) Data were obtained from co-migration experiments.

For triplexes which we classified as 'stable' in our previous work (with T_m identical or even higher than the T_m of the corresponding target duplex) (12,24) it was reasonable to suggest that oligonucleotides complementary to a part of the TFO could be pushed out during the interaction of the TFO with the targeted duplex. Moreover, one can expect that this partial duplex can protect purine-rich oligonucleotides from self-association. We have named these structures 'zipper' oligonucleotides. We have tested different oligonucleotides, matching different parts of the 20mer TFO. It was found that even three residues in a single-stranded form at 3′-end of the 'zipper' TFO are sufficient to provoke slow triplex formation with the targeted sequence. Increase of the length of the single-stranded part leads to a substantial increase in the rate of triple-helix formation. As one sees in Figure 5A, triplexes formed by the 20mer alone and by 'zipper' oligonucleotide are qualitatively different. In the case of the 20mer alone, only the stretch of the first five guanines is protected in DMS footprint experiments. We were unable to get full protection of guanines even at 10 μM concentration of VPX20. The footprint of the triplex formed by the 'zipper' oligonucleotide shows a much more uniform protection of the guanines within the targeted sequence. This indicates that the reaction of triplex formation proceeds as predicted: the single-stranded part of the 'zipper' oligonucleotide finds the target followed by the quick zipping of the triplex-forming oligonucleotide with the targeted DNA and the pushing-out of the complementary part of the 'zipper' oligonucleotide.

Recently, Gee *et al.* (25) and Olivas and Maher (7) suggested an alternative approach to overcome potassium-mediated inhibition of triplex formation. They have developed oligonucleotides, containing 6-thioguanine bases substituted for part of the guanines in the TFOs. These TFOs were resistant to potassium-mediated aggregation, yet were still able to form stable triplexes. The principal difference between this and our approach is the absence of modified bases in our TFO.

Based on these results one may explain the 'optimal length' for target binding obtained with a 12mer purine TFO in DNAse footprint experiments (8). It seems very likely that in the case of long oligonucleotides the decrease in their ability to form triplexes might be due to the oligonucleotide self-association. The 'zipper' oligonucleotide approach presents the first attempt to overcome potassium inhibition of triplex formation for oligonucleotides composed of unmodified purine bases. It seems likely that this strategy may prove useful for triple-helix based gene targeted therapy.

ACKNOWLEDGEMENTS

We thank Dr E. Lescot for oligonucleotides synthesis. We are very thankful to Dr J. Paoletti for the software of T_m recording and Drs T. O'Conner and L. Pritchard for the helpful discussion. This work was supported by the 'Agence Nationale de Recherches sur le SIDA' research fellowship to F.S.; by INSERM grant no. 94 EO 08 and by le Ministère de l'Enseignement Supérieur et de la Recherche and l'Institut de Formation Supérieure Biomédicale research fellowship to A.D. and by the Programme Internationale de Cooperation Scientifique PICS no. 227 to D.C.

REFERENCES

1 Behe,M.J. (1995) *Nucleic Acids Res.*, **23**, 689–695.
2 O'Neill,D., Bornschlegel,K., Flamm,M., Castle,M. and Bank,A. (1991) *Proc. Natl. Acad. Sci. USA*, **88**, 8953–8957.
3 Grigoriev,M., Praseuth,D., Guieysse,A.L., Robin,P., Thuong,N.T., Helene,C. and Harel-Bellan,A. (1993) *Proc. Natl. Acad. Sci. USA*, **90**, 3501–3505.
4 Wang,G., Seidman,M. and Glaser,P. (1996) *Science*, **271**, 802–805.
5 Moser,H.E. and Dervan,P.B. (1987) *Science*, **238**, 645–650.
6 Beal,P.A. and Dervan,P.B. (1991) *Science*, **251**, 1360–1363.
7 Olivas,W.M. and Maher,L.J. (1995) *Nucleic Acids Res.*, **23**, 1936–1941.
8 Olivas,W.M. and Maher,L.J. (1995) *Biochemistry*, **34**, 278–284.
9 Suda,T., Mishima,Y., Asakura,H. and Kominami,R. (1995) *Nucleic Acids Res.*, **23**, 3771–3777.
10 Noonberg,S.B., Francois,J.-C., Garestier,T. and Helene,C. (1995) *Nucleic Acids Res.*, **23**, 1956–1963.
11 Svinarchuk, Bertrand,J.-R. and Malvy,C. (1994) *Nucleic Acids Res.*, **22**, 3742–3747.
12 Svinarchuk,F., Monnot,M., Merle,A., Malvy,C. and Fermandjian,S. (1995) *Nucleic Acids Res.*, **23**, 3831–3836.
13 Svinarchuk,F., Debin,A., Bertrand,J.-R. and Malvy,C. (1996) *Nucleic Acids Res.*, **24**, 295–302.
14 Puglisi,J.D. and Tinoco,I.,Jr, (1989) *Methods Enzymol.*, **180**, 304–335.
15 Sambrook,J., Fritsch,E.F. and Maniatis,T. (1989) In *Molecular Cloning: A Laboratory Manual.* 2nd Edn, vol.1, p.1.42, SCH Press, USA.
16 Cherny,D.I., Malkov,V.A., Volodin,A.A. and Frank-Kamenetskii,M.D. (1993) *J. Mol. Biol.* **230**, 379–383.
17 Cherny,D.I., Kurakin,A., Lyamichev,V., Frank-Kamenetskii,M., Zinkevich,V., Firman,K. and Nielsen,P. (1994) *J. Mol. Recogn.*, **7**, 171–176.
18 Dubochet,J., Ducommun,M., Zollinger,M. and Kellenberger,E. (1971) *J. Ultrastruct. Res.*, **35**, 147–167.
19 Delain,E., Fourcade,A., Revet,B. and Mory,C. (1992) *Microsc. Microanal. Microstruct.*, **3**, 175–186.
20 Delain,E. and Le Cam,E. (1995) In Gérald Morel (ed.) *Visualisation of Nucleic Acids.* CRC Press, pp. 35–56.
21 Voloshin,O.N., Mirkin,S.M., Lyamichev,V.I., Belotserkovskii,B.P. and Frank-Kamenetskii,M.D. (1988) *Nature*, **333**, 475–476.
22 Demidov,V.V., Yavnilovich,M.V., Belotserkovskii,B.P, Frank-Kamenetskii,M.D. and Nielsen,P.E. (1995) *Proc. Natl Acad. Sci. USA*, **92**, 2637–2641.
23 Cheng,A. and Van Dyke,M. (1993) *Nucleic Acids Res.*, **21**, 5630–5635.
24 Svinarchuk,F., Paoletti,J. and Malvy,C. (1995) *J. Biol. Chem.*, **270**, 14068–14071.
25 Gee,J.E., Revankar,G.R., Rao,T.S. and Hogan,M.E. (1995) *Biochemistry*, **34**, 2042–2048.